JOURNAL OF MATERIALS SCIENCE 13 (1978) 1455–1463

The structure of slow crack interfaces in silicon nitride

N. J. TIGHE
National Bureau of Standards, Center for Materials Science, Washington, DC 20234, USA

Fracture interfaces formed in silicon nitride at high temperatures were studied using light and electron microscopy. The structure of the fracture interface depended on the type of silicon nitride fractured. High-purity, reaction-bonded silicon nitride always formed flat, relatively featureless, fracture surfaces. Fracture occurred by a brittle mode even at the highest temperature (1500° C) studied. The critical stress intensity factor for reaction-bonded silicon nitride (~ 2.2 MN $m^{-3/2}$) is relatively low and is insensitive to temperature. By contrast, hot-pressed silicon nitride gave evidence of plastic flow during fracture at elevated temperatures. Crack growth in magnesia-doped, hot-pressed silicon nitride occurs by creep, caused by grain boundary sliding and grain separation in the vicinity of the crack tip. As a consequence of this behaviour, extensive crack branching was observed along the fracture path. The primary and secondary cracks followed intergranular paths; sometimes dislocation networks, generated by momentary crack arrest, were found in grains bordering the crack interface. As a result of the high temperature, cracks were usually filled with both amorphous and crystalline oxides that formed during the fracture studies. Electron microscopy studies of the compressive surfaces of four-point bend specimens gave evidence of grain deformation at high temperatures by diffusion and dislocation motion.

1. Introduction

Hot-pressed and reaction-bonded silicon nitride materials are being developed for use in gas turbine engines which have service temperatures as high as 1400° C. The strength and fracture toughness data obtained for these materials show that most currently available compacts may not be useful because their strength degrades during exposure to such temperatures [1–7]. In order to improve the high temperature behaviour, it is essential to understand why the strength and fracture toughness degrade during high temperature exposures and why the two types of silicon nitride behave differently.

Although the strength of magnesia-doped hot-pressed silicon nitride (HPSN) is two to three times greater than reaction-bonded silicon nitride (RBSN) at 25° C, the strength of reaction-bonded silicon nitride changes little with exposure to high temperature, while that of hot-pressed silicon nitride degrades at temperatures above ~ 1200° C. At 1400° C the strength of both materials is ~ 250 MPa. From measurements of crack velocity and fracture toughness Lange [5], and Evans and Wiederhorn [4] correlated the strength degradation of magnesia-doped hot-pressed silicon nitride with the onset of slow crack growth. They suggested that slow crack growth occurred as a result of plastic deformation or stress corrosion in the neighbourhood of the crack tip. Reaction-bonded silicon nitride did not exhibit slow crack growth under similar test conditions.

In this paper we characterize fracture and slow crack growth and the strength degradation in terms of the microstructural changes which occurred in 4-point bend and double torsion specimens during experiments at 1400° C. The fracture interfaces and the regions near fracture interfaces in these

specimens were examined by light and electron microscopy. Earlier microscopy studies [8, 9] showed that hot-pressed silicon nitride was composed primarily of blocky α-Si_3N_4 grains ($\sim 1\,\mu m$ diameter) and column-like β-Si_3N_4 grains ($\sim 1\,\mu m \times 5\,\mu m$). In addition, it contained micron-sized grains of α- and β-SiC, and Si_2N_2O. Furthermore, glass was occasionally found at triple junctions and as micron-sized regions. The microstructure is therefore heterogeneous with respect to composition. The reaction-bonded silicon nitride [10] was composed of ultra-fine α-Si_3N grains ($\sim 0.02\,nm$) and larger β-Si_3N_4 and SiC grains (~ 1 to $5\,\mu m$). The SiC phases occurred in both materials because they were hot-pressed or reaction-bonded in a carbonaceous atmosphere. Both materials oxidized at the test temperature; a complex crystalline and amorphous oxide layer was formed on the surface [11].

2. Experimental procedure

2.1. Materials

The hot-pressed and the reaction-bonded silicon nitride materials examined in this study are currently under consideration for turbine engine applications. Two hot-pressed compositions* (HS130 and NC132) of magnesia-doped Si_3N_4 were obtained in the form of billets 75.5 cm x 75.5 cm x 2.5 cm. The manufacturer listed the following impurities (wt%): 0.20 Al, 0.05 Ca, 0.40 to 0.64 Fe, 0.70 to 0.74 Mg, 2.6 to 2.7 W. Two sets of reaction-bonded silicon nitride specimens (NC350) were obtained as plates 7.6 cm x 2.5 cm x 0.2 cm. Test specimens were cut from the billets and ground into plates 7.6 cm x 2.5 cm x 0.2 cm for double-torsion tests and into bars 5.5 cm x 1.0 cm x 5.5 cm for 4-point bend tests. The double-torsion specimens were grooved along their length by sawing through approximately 1/2 the plate thickness. The specimens were notched at one end of the groove.

2.2. Mechanical testing

Stress intensity factors and crack velocity data were obtained on the double-torsion specimens using the procedure for propagating a controlled crack at high temperature as used by Evans [7]. In this method, the grooved and pre-cracked double-torsion specimens (Fig. 1) were held in a silicon carbide jig with the grooved side up. The load was applied at a constant displacement rate to a ram,

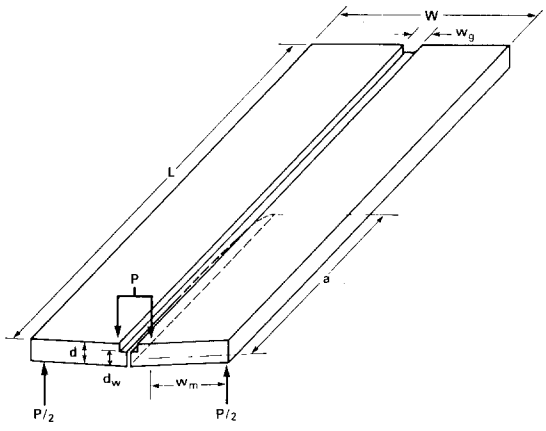

Figure 1 Schematic diagram of a double-torsion specimen showing the saw groove (Wg) and the notch at one end. The load is applied at P and the crack is drawn as a dashed line.

which straddled the central notch at P. The load was increased until the critical stress for crack initiation occurred and the crack propagated along the groove at constant load. Displacement rates from 5×10^{-5} to $5 \times 10^{-2}\,cm\,min^{-1}$ were used. The stress intensity factors were calculated from the load and specimen dimensions. The crack velocity was obtained from measurements of the crack length as a function of time at constant load. Very low crack velocities were obtained by applying a constant load for fixed time intervals up to 48 h. Crack lengths that were measured using a fluorescent dye penetrant were in good agreement with measurements of the crack tip displacement after the plate was broken into two parts.

2.3. Microscopy

Transverse and parallel sections of the test specimens were examined using light and electron microscopy. Specimens were prepared for transmission electron microscopy by standard ion thinning procedures [12]. In this method, disks 3 mm in diameter were cut from polished thin plates 50 to $100\,\mu m$ thick, using a diamond core drill. These disks were then polished to a thickness of approximately $50\,\mu m$ and ion-thinned using argon ions. Copper single-hole grids were cemented onto the specimens with epoxy cement to strengthen and to support the thin foil. The thin foils were examined in an electron microscope operating at 200 kV. The double-torsion specimens and the bend specimens were examined with a light microscope in

*The Si_3N_4 materials were obtained from the Norton Co., Boston, Mass, USA.

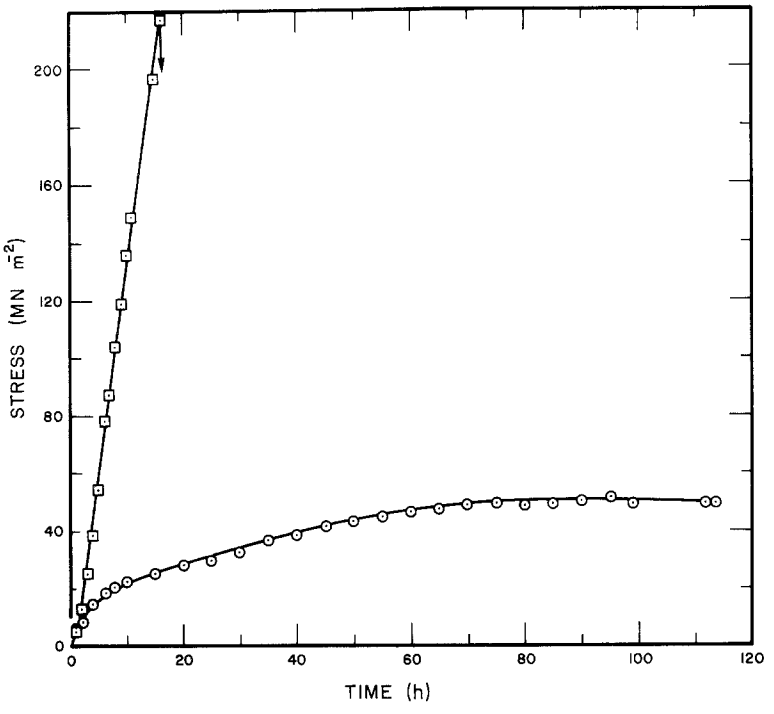

Figure 2 Strength versus stressing time for hot-pressed silicon nitride (○) and reaction-bonded silicon nitride (□) tested in 4-point bending.

order to establish the macroscopic characteristics of the deformation, and to compare the electron microscopy results with these features.

3. Results

3.1. Mechanical properties

The hot-pressed silicon nitride and reaction-bonded silicon nitride, behaved differently during the mechanical tests. In the 4-point bend tests, hot-pressed silicon nitride deformed plastically and exhibited secondary creep at 1400° C, whereas, reaction-bonded silicon nitride deformed elastically to failure at approximately 212 MN m^{-2} at 1500° C. Curves showing the calculated stress versus time for these two materials are shown in Fig. 2. The load was applied at the displacement rate of 8.5 × 10^{-9} m sec^{-1}.

The stress intensity factor K_I obtained for hot-pressed silicon nitride showed distinct temperature dependence. The stress intensity versus crack velocity results obtained for NC 132 at 1400° C and at 1200° C are plotted in Fig. 3. The variation in K_I with crack velocity shows that extensive slow crack growth occurred at 1400° C. At 1200° C slow crack growth was minimal as indicated by the change in slope of the $K-V$ plot. Reaction-bonded silicon nitride did not exhibit slow crack growth at 1400° C and at this temperature K_I was ~ 2.2 MN m$^{-3/2}$ over the range of loading rates used for the tests.

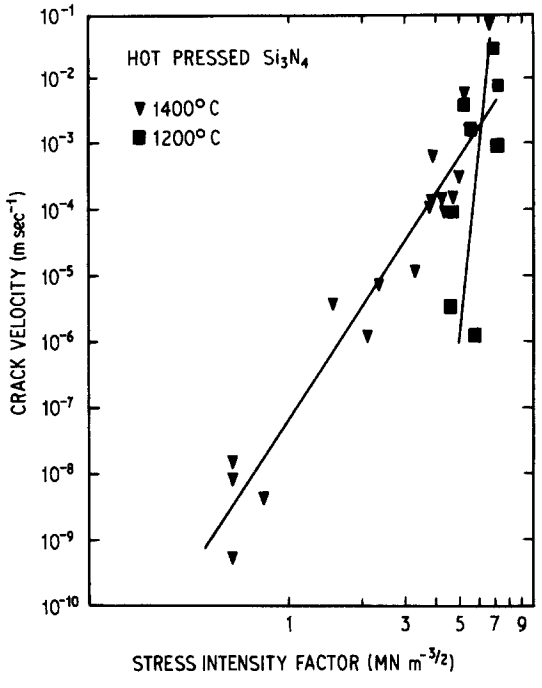

Figure 3 K, V data for silicon nitride tested in air at 1200° C and 1400° C.

3.2. Fracture interfaces

3.2.1. Light microscopy

The hot-pressed silicon nitride double-torsion specimens bent plastically during crack growth experiments at 1400° C. This deformation and

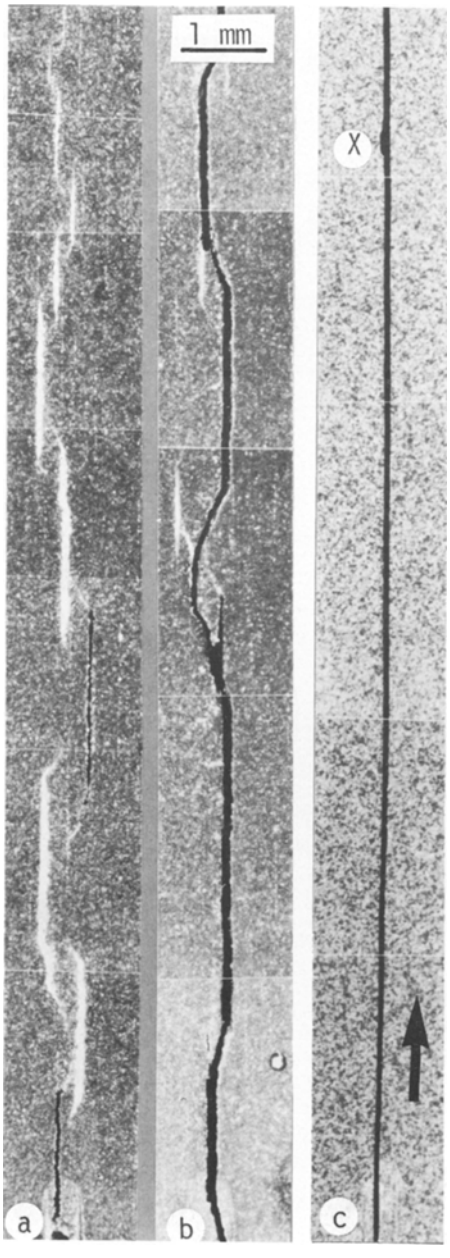

Figure 4 Light micrographs of the tension sides of double-torsion specimens tested at 1400° C: (a), (b) hot-pressed silicon nitride, (c) reaction-bonded silicon nitride. Cracks propagated in the direction of the arrow.

subsequent oxidation of the surfaces kept the crack interfaces separated along the tension surface after the stresses were removed. The path of the primary crack was therefore outlined by oxide and was easy to see. In Fig. 4a, it can be seen that the primary crack oscillated along the groove and, at successive intervals, the tips of the crack segments overlapped. The oscillations occurred as the crack

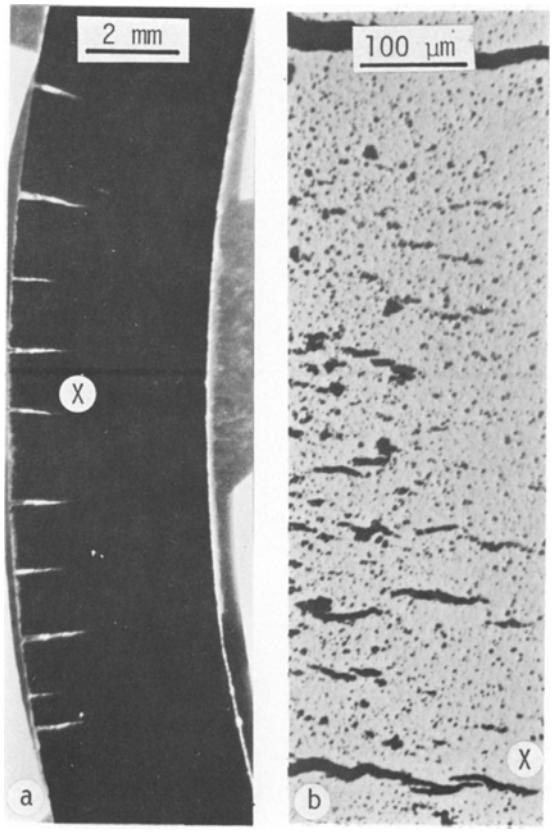

Figure 5 Light micrograph of a hot-pressed silicon nitride specimen deformed in 4-point bending at 1400° C: (a) polished section of specimen, (b) details around crack tips.

propagated and were not related to the crack arrest at the end of each experiment. In specimens which were broken into 2 pieces the overlapping crack tips were torn apart as illustrated in Fig. 4b.

In contrast with the hot-pressed material the reaction-bonded silicon nitride specimens did not deform at temperatures as high as 1500° C. Slow crack growth did not occur and the fracture interfaces were nearly featureless. Some disruption in the surface occurred at the crack origins as at X in Fig. 4c.

Further evidence for the tearing apart of the structure of the hot-pressed silicon nitride during deformation was found by examining 4-point bend specimens after polishing away the surface oxide. The unnotched specimen shown in Figs. 5a and b was bent uniformly across the gauge length. Cracks which grew along the machined edges of the tension side of the specimen penetrated up to 1 mm deep. However, near the middle of the tension surface of the bar, cracks were only 0.1 mm deep, thus demonstrating the strong corner effect of the

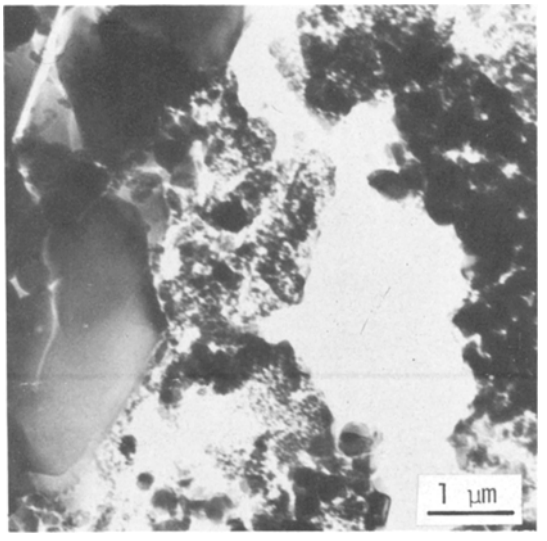

Figure 6 Electron micrograph of a section from double-torsion specimen showing oxide along the primary crack.

crack nucleation. As seen in the figure the surface and sub-surface cracks were filled with oxide which enhanced the crack visibility in polished sections.

It is clear that the crack branching characteristics of slow cracks in hot-pressed silicon nitride and the smooth interfaces of rapid cracks in reaction-bonded silicon nitride can be distinguished by light microscopic examination of the specimens. However, the grain size in both materials is small and cannot be resolved by light microscopy. Therefore, the relations between the cracks and the microstructure can be determined only by electron microscopy.

3.2.2. Electron microscopic examination

Areas around the primary cracks in hot-pressed silicon nitride specimens tested at 1400° C were examined by electron microscopy using thin foils made from sections cut parallel to the length of the cracks. As expected from the light microscopy, the primary crack shown in Fig. 6 had oxide along its interfaces. Near the primary crack tips many intergranular cracks several micrometres long were found which were arranged approximately parallel to the primary crack. From the array shown in Fig. 7 it is apparent that the compact was pulled apart along grain boundaries. The fine structure of cracks is similar to the crack branching macrostructure seen in the light micrographs.

The oxides on the crack surfaces can form by oxidation of the crack interfaces during fracture. Furthermore the cracks which are held open because of the deformation can be filled by migration of the oxide formed on the specimen surfaces, and from the silicate phase in the matrix.

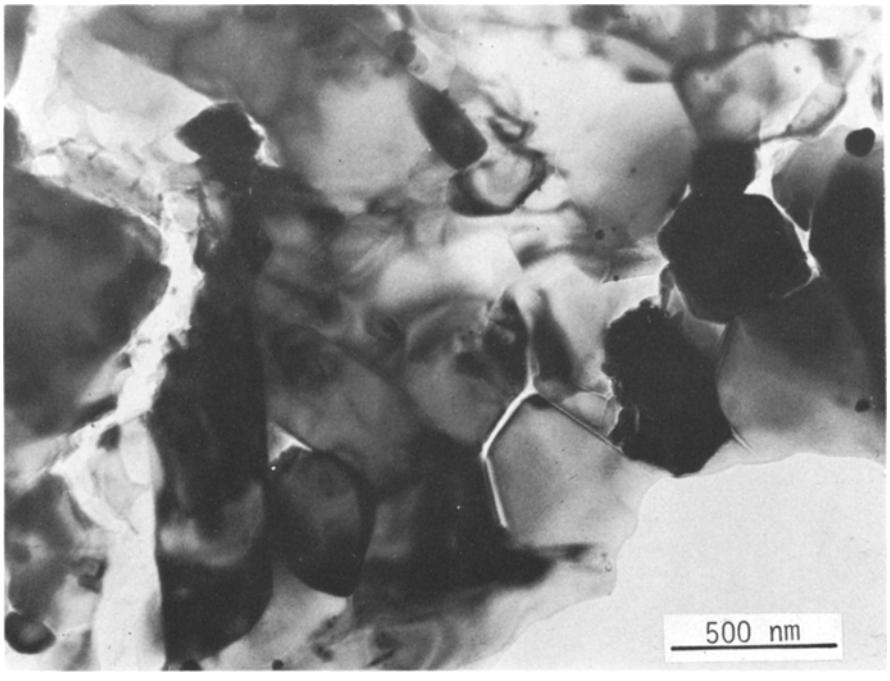

Figure 7 Secondary cracks arrayed approximately parallel to the primary crack. Note that the cracks follow the grain boundaries.

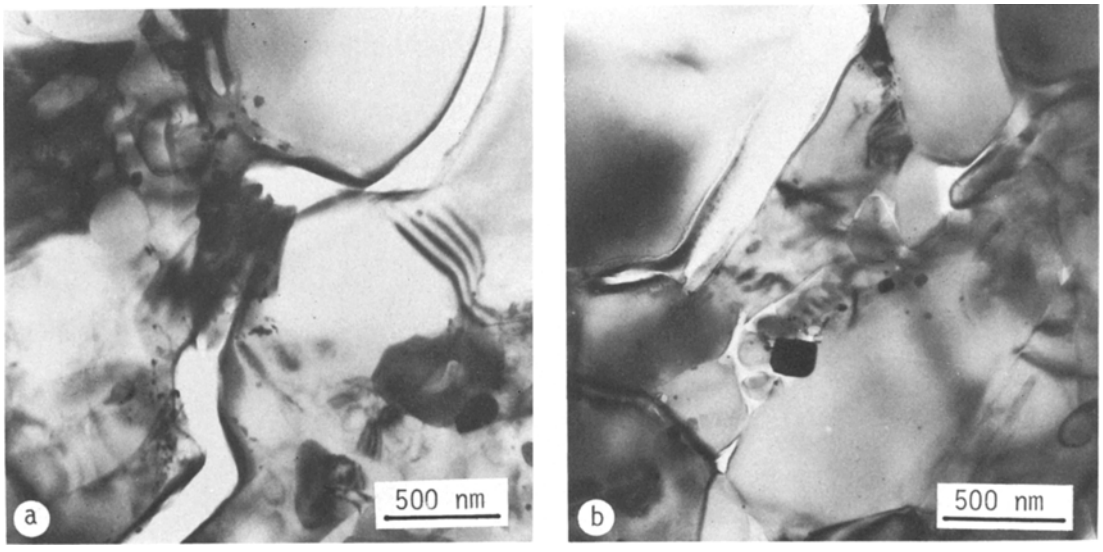

Figure 8 Secondary cracks near primary crack in a double-torsion specimen tested at 1400° C: (a) crack 3 to 4 grain diameters long, (b) cracks and pores nearly filled with amorphous phase.

Examples of cracks which have oxide along the interfaces are seen in Fig. 8. An amorphous phase was found also in pores and in open cracks of this specimen. These amorphous phases had electron diffraction patterns similar to the patterns taken of SiO_2 in other oxidized silicon nitride specimens [11].

When the grain boundary crack shown in Fig. 8a was followed to its tip, dislocation arrays were found in the grains adjacent to the crack tip (Fig. 9). It appears that this crack propagated along the grain boundaries and, when it arrested, the strain release produced dislocation pile-ups on both sides of the crack tip. In grain A, the dislocations have formed in a network approximately parallel to the basal plane, and their presence indicates that plastic deformation occurred within these grains at 1400° C.

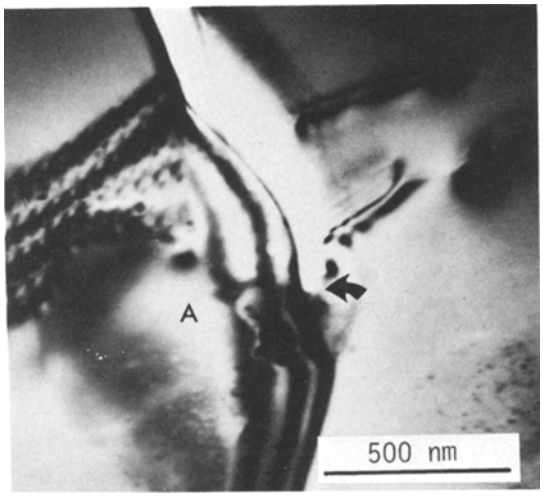

Figure 9 Tip of grain boundary crack in Fig. 8a showing dislocation arrays extending into adjacent grains.

The microstructure of the reaction-bonded material as shown in Fig. 10 was considerably different from the microstructure of the hot-pressed material. The structure was bi-modal with a fine-grained α-phase 10 to 20 nm in diameter, and a β-phase. Some large grains of silicon carbide were found also and these grains and the β-silicon nitride grains were usually faulted. The images of the small α-grains in Fig. 10b overlapped and gave a very confused picture; however, individual grains can be distinguished by the presence of moiré fringes from overlapping grains. There was little difference in microstructure between as-received and tested specimens except at the surface where a thin layer of β-cristobalite and glass had formed during the experiments. This observation suggests that the microstructure of the reaction-bonded material was not affected by the stress.

In the hot-pressed specimens, which were bent at 1400° C, grains near the tension side were pulled apart at grain boundaries in a manner similar to grains in the double-torsion specimens. Extensive fragmentation occurred near the silicon nitride–oxide interfaces and the cracks near this interface were filled with oxide. Thin foil specimens which were made from the tension side of the bend bars were extremely fragile and some areas were lost in handling.

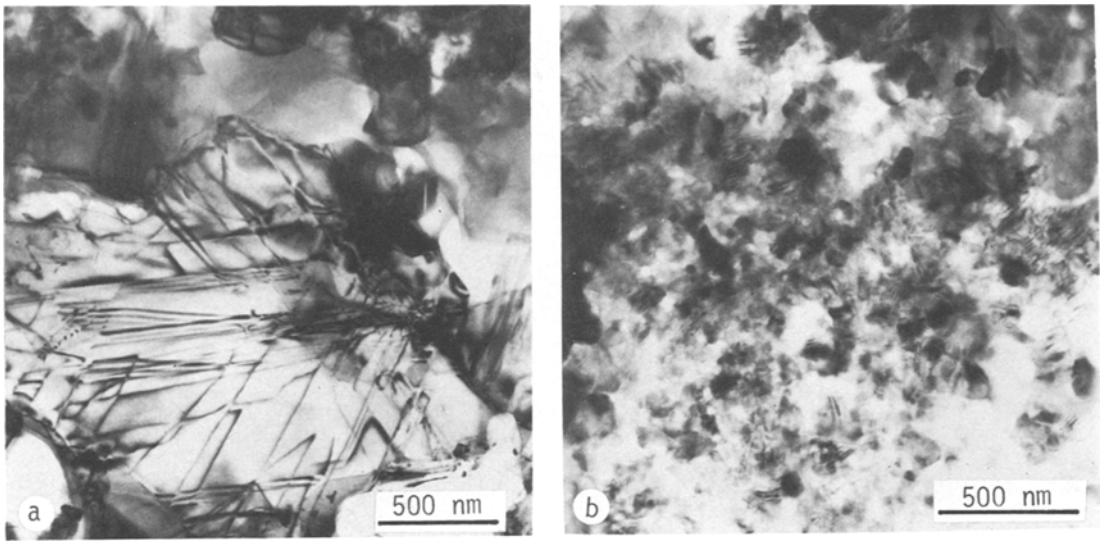

Figure 10 Reaction-bonded silicon nitride showing: (a) fine grains of α-Si_3N_4 and large grains of β-Si_3N_4 and β-SiC, (b) α-grains.

In specimens taken from the compression side of the bend bar it was found that most grains had extensive dislocation arrays which were associated with grain boundaries as in Figs. 11a and b. When stereopairs were taken of the area in Fig. 11a it appeared that the dislocations left the grain boundary, interacted with small particles, and then broke up into loops. Since these dislocation interactions were not found in as-received specimens, this dislocation motion must have occurred in the grains as a result of bending. Extensive arrays of bubbles near grain boundaries also were found only in foils made from the compression side of the bent bars (Fig. 11c). These bubbles were found in undulating arrays which were displaced slightly from the grain boundaries in some grains and in the centre of other grains. Such arrays are suggestive of diffusion along the grain boundary or movement of the grain boundary during compression. Such bubble formation was not found in the silicate regions shown in Figs. 6 and 8. The bubbles were observed in most grains and could not be associated with any degradation resulting from electron beam irradiation. Clusters of small defect-free grains, as shown in Fig. 11d, also were found in foils made from the compression side. These microstructural changes are manifestations of plastic deformation, diffusion recrystallization and grain growth, which occurred on the compression side of bars bent at 1400° C.

4. Discussion

The microscopic analysis presented above suggests that the differences in fracture toughness between the hot-pressed silicon nitride and the reaction-bonded silicon nitride can be related to the differences in microstructure between these two materials. The MgO and CaO based additives promoted sintering and densification during hot pressing at temperatures near 1700° C. As a result, the grain size distribution is more homogeneous but more crystalline and amorphous second phases are present in hot-pressed material than in reaction-bonded silicon nitride. The reaction-bonded material did not have additives and was porous and had a bi-modal grain size distribution. A crack in reaction-bonded silicon nitride traversed the weakly sintered matrix easily because it encountered only ultra-fine grains, pores and large faulted grains. A crack in hot-pressed silicon nitride encountered well-sintered grains and propagated intergranularly, indicating that grain boundaries presented easy but more tortuous fracture paths. The micrographs taken from specimens fractured at 1400° C showed that slow crack growth was enhanced by plastic deformation in regions surrounding the crack tip and that the grain boundaries were pulled apart over a considerable distance. The dislocations that were observed along grain boundaries and within grains in MgO-doped hot-pressed silicon nitride are evidence for some localized plastic deformation.

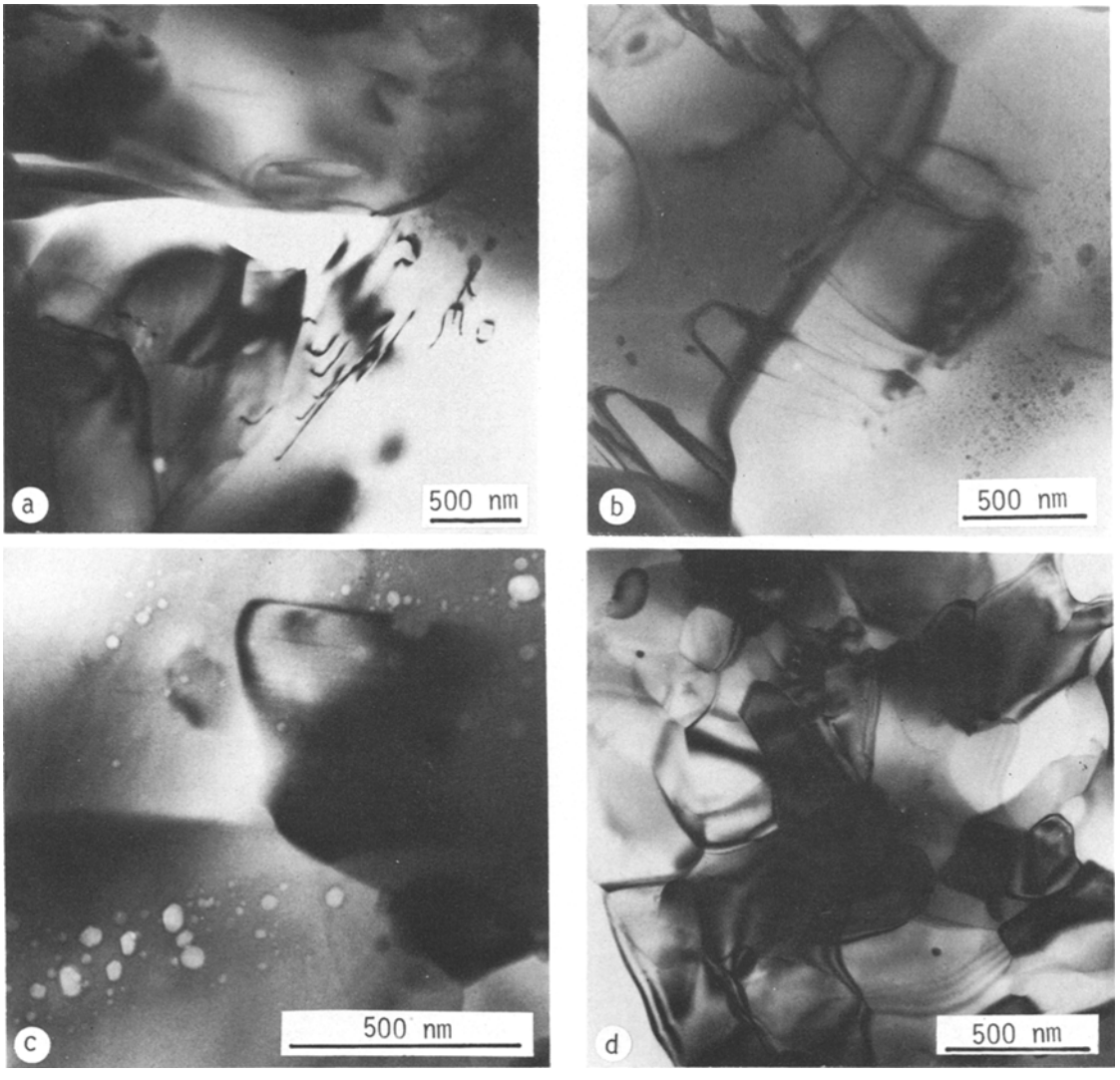

Figure 11 Regions near compression side of specimen bent at 1400° C: (a) and (b) dislocations and faults interacting at grain boundaries (c) array of pores forming "ghost" boundary, (d) recrystallized grains.

Oxides were observed along fracture interfaces and along some grain boundaries in the neighbourhood of the cracks and could be evidence for grain boundary sliding.

The strength degradation that is observed in hot-pressed silicon nitride has been attributed to grain boundary sliding involving shear deformation of a thick (~ 100 nm) glass phase between grains [5, 6]. This type of grain boundary sliding could occur without plastic deformation of the grain. Although micro-probe analysis by Kossowsky [13] showed that magnesium and calcium segregated near grain boundaries a significant amount of glass phase (> 3 nm thickness) has not been found by electron microscopy at grain boundaries in undeformed commerical materials. In most of the micrographs shown in this paper, the silicon nitride grains were sintered together and an amorphous phase could not be resolved between grain boundaries before fracture. Glass phases were detected at triple junctions and as distinct separate regions several hundred nanometers in diameter. Recently, Clarke and Thomas [14], using high resolution electron microscopy obtained lattice images of grains and detected a phase which was $\sim\frac{1}{2}$ nm wide between grains and wider at triple junctions.

The contribution of the crystalline or amorphous silicate phases to high temperature deformation can be illustrated by considering that at 1400° C,

magnesium silicate has the viscosity of water, and although pure silica glass has a higher viscosity, many of the possible Mg and Ca silicate phases can melt and thus be very mobile at such temperatures. With a liquid phase present, grain boundary sliding could cause the dislocation arrays observed here by a mechanism akin to abrasion and wear on lubricated surfaces. Thus grain boundary sliding does not necessarily require a 100 nm thick phase between grains when the magnesium based sintering aid can melt or otherwise decompose and when deformation can occur within the grains and along grain boundaries. Grains under a tensile or shear stress can simply pull apart and grains under compressive stress can accommodate the strain by diffusional creep. The bubbles and dislocation arrays observed near grain boundaries support this concept of localized deformation in the bent specimens. Rapid diffusion of impurities at 1400° C is shown by the presence of Mg and Ca in the outer oxide layer. The exact composition of the oxide phase is a function of the exposure time [11].

The reaction-bonded silicon nitride did not deform plastically in the present experiments and analysis of this deformation mode in reaction-bonded silicon nitride could not be made. Thin foil specimens made from a series of extensively deformed samples of both hot-pressed and reaction-bonded silicon nitride must be examined before the deformation mode can be defined completely. Silicon nitride dissociates without melting, and oxidizes or reduces depending on the surrounding atmosphere. It will be necessary, therefore, to do tests in vacuum and nitrogen as well as in air.

5. Conclusions

By examining specimens from double-torsion, fracture mechanics tests and from 4-point bend tests, we have shown that in hot-pressed silicon nitride: (1) extensive crack branching occurred in specimens fractured or bent at 1400° C; (2) slow crack growth observed in high temperature tests resulted from plastic deformation; (3) this plastic deformation occurred by grain boundary sliding which involved both slip along grain boundaries and within grains, and separation of grains through reaction with the silicate phase. Reaction-bonded silicon nitride deformed elastically under the same conditions. The difference in high temperature strength and fracture toughness between hot-pressed and reaction-sintered silicon nitride was related to compositional and microstructural differences between the materials.

Acknowledgement

The author gratefully acknowledges the support of the Air Force Materials Laboratory.

References

1. A. G. EVANS and R. W. DAVIDGE, *J. Mater. Sci.* 5 (1970) 314.
2. W. ASHCROFT, "Ceramics for Turbines and Other High-Temperature Engineering Applications", (British Ceramic Society, Stoke-on-Trent, 1973). p. 169.
3. M. L. TORTI, R. A. ALLIEGRO, D. W. RICHERSON, M. E. WASHBURN and G. Q. WEAVER, *ibid* p. 129.
4. A. G. EVANS and S. M. WIEDERHORN, *J. Mater. Sci.* 9 (1974) 270.
5. F. F. LANGE, *J. Amer. Ceram. Soc.* **57** (1974) 84.
6. R. KOSSOWSKY, D. G. MILLER, and E. S. DIAZ, *J. Mater. Sci.* **10** (1975) 983.
7. A. G. EVANS, "Ceramics for High-Performance Applications", edited by J. J. Burke, A. E. Gorum and R. N. Katz (Brook Hill, Mass., 1974) p. 373.
8. P. DREW and M. H. LEWIS, *J. Mater. Sci.* 9 (1974) 261.
9. N. J. TIGHE, "Nitrogen Ceramics," edited by F. Riley (Noordhoff, Leyden, 1977) p. 441.
10. A. G. EVANS and J. V. SHARP, *J. Mater. Sci.* 6 (1971) 1292.
11. N. J. TIGHE, Proceedings of the Electron Microscopy Society of America, Vol. 32 (Claitors Publishing Co., Baton Rouge, La., 1974) p. 470.
12. *Idem*, "Electron Microscopy in Mineralogy", edited by H. -R Wenk (Springer-Verlag, Berlin, 1976) p. 144.
13. R. KOSSOWSKY, *J. Mater. Sci.* 8 (1973) 1603.
14. D. R. CLARKE and G. THOMAS, *J. Amer. Ceram. Soc.* **60** (1977) 491.

Received 10 May and accepted 19 October 1977.